A TECHNIQUE FOR SMOOTH TRANSFORMATION OF LARGE-SCALE ANALYSES ONTO A HIGH RESOLUTION GRID

D. Majewski
Deutscher Wetterdienst
Offenbach a.M., FR Germany

1. INTRODUCTION

The highest resolution of present day global numerical weather prediction models is about 190 km half wavelength (ECMWF,T106). These models are capable of covering the synoptic development up to 4 or 5 days ahead with sufficient reliability (Bengtsson, 1984).

However, there are important systems of atmospheric motion which are not adequately resolved (Atkinson, 1981):

- Structures which are strongly forced by small-scale features at the surface, such as orographic waves, land/sea breeze circulations,
- Strong horizontal and vertical gradients which may be found at the jet level, near fronts, and in the atmospheric boundary layer,
- Small lows and waves at fronts and in the pool of cold air characterizing a cold outbreak,
- Organized convection, e.g. meso-scale convective complexes.

Meteorological guidance for dealing with these phenomena is drawn from meso-scale numerical models with a horizontal grid mesh of 10 to 100 km. Due to the limited storage and speed of existing computers, the meso-scale models are restricted in their horizontal (and sometimes vertical) extent to that region of the globe for which detailed forecasts are wanted. Such limited area models (LAM) require the specification of appropriate initial and boundary values. To obtain a good short-range forecast with a LAM, balanced initial and boundary fields are necessary to avoid unwanted gravity waves in the forecast,

which form due to initial imbalances and noisy boundary data (Kallberg, 1977; Miyakoda and Rosati, 1977).

Although the full advantage of a meso-scale forecast is realizable only by initializing the model with a detailed meso-scale analysis, a good part of the high resolution information can be obtained using interpolated large-scale analyses as initial values. The LAM itself generates meso-scale motion systems due to differential forcing by the underlying surface and scale interactions.

This paper describes the techniques for a smooth transformation of large-scale analyses onto a LAM's grid and discusses the problem of spin-up time for meso-scale structures in the forecast. The large-scale analysis used is the initialized ECMWF-analysis on model levels, DATA- and DATB-series (Lorenc, 1981), but the method is generally applicable to any large-scale analysis or forecast. We interpolate the initialized ECMWF-analysis (hereafter EC) on the grid of the "Europa-Modell" (hereafter EM), which is an experimental meso-scale model of the Deutscher Wetterdienst.

Difficulties usually arise if the orographies of the large-scale model and the LAM differ considerably. To avoid the interpolation problem in such a case, some modellers (Dell'Osso, 1983) start the forecast with the smoother large-scale orography and introduce the steeper LAM-mountains gradually during the first twelve hours of the forecast. This approach seems unsatisfactory because the useful forecasting range of the LAM is shortened. At least the first twelve hours are lost, a very important period for short-range forecasts. Other investigators (Hoke, Phillips and Sela, 1983) interpolate the initialized fields only horizontally, but use the same vertical levels as the global model. This avoids the problem of vertical interpolation but precludes the introduction of a fine-scale orography, which is an important forcing factor in meso-scale models. This paper describes a method for horizontal and vertical interpolation of initialized global analyses onto a LAM's-grid which conserves the balanced properties of the global analyses.

2. GRID STRUCTURES OF THE MODELS

2.1 The EC-model

The operational EC-model from 1979 to 1983 was the N48 gridpoint model. The grid was Arakawa C-type with a latitude/longitude discretisation of 1.875^{o} in both directions, i.e. 192 gridpoints in the zonal, 97 gridpoints in the meridional direction for the global model. The vertical coordinate was $\sigma = p/p_s$ (p_s: surface pressure) with 15 unequally spaced levels, see Table 1a.

From April 21, 1983 till April 30, 1985 the ECMWF ran a spectral model truncated at total wavenumber 63 (T63) with 16 hybrid vertical levels, see Table 1b.

On May 1, 1985 the ECMWF introduced the T106 spectral model with the same 16 vertical levels as the T63 model. The forecasts presented in this paper are based on interpolated N48 and T63 initialized analyses.

Table 1a Vertical levels of the ECMWF N48 gridpoint model(1982)

K	σ	p(hPa)
1	0.0251	25.1
2	0.0766	76.6
3	0.1319	131.9
4	0.1928	192.8
5	0.2601	260.1
6	0.3342	334.2
7	0.4145	414.5
8	0.5000	500.0
9	0.5888	588.8
10	0.6782	678.2
11	0.7651	765.1
12	0.8454	845.4
13	0.9144	914.4
14	0.9666	966.6
15	0.9960	996.0
p for p_s = 1000 hPa		

Table 1b Vertical levels of the ECMWF T63 spectral model (1984)

K	p(hPa)
1	25.0
2	72.4
3	125.8
4	183.6
5	248.7
6	322.6
7	405.0
8	494.3
9	587.4
10	680.4
11	768.2
12	845.9
13	909.0
14	954.7
15	982.6
16	996.1
p for p_s= 1000 hPa	

2.2 The EM-model

The "Europa-Modell" covers Europe, the East Atlantic and North Africa. It has 73 x 69 gridpoints (cartesian coordinates) on a polar stereographic projection with a grid size of 63.5 km at 60°N. The resolution ratio of the EC-models N48, T63 to the EM-model is thus approximately 3:1. The hybrid vertical coordinate consists of 3 pressure levels above 15 sigma levels (Table 2).

Table 2 Vertical levels of the "Europa Modell" (1983)

K	p; σ	p (hPa)
1	50.0	50.0
2	137.5	137.5
3	212.5	212.5
4	0.050	288
5	0.150	363
6	0.250	438
7	0.350	513
8	0.450	588
9	0.550	663
10	0.635	726
11	0.705	779
12	0.770	828
13	0.825	869
14	0.875	906
15	0.920	940
16	0.955	966
17	0.980	985
18	0.995	996
p for p_s = 1000 hPa		

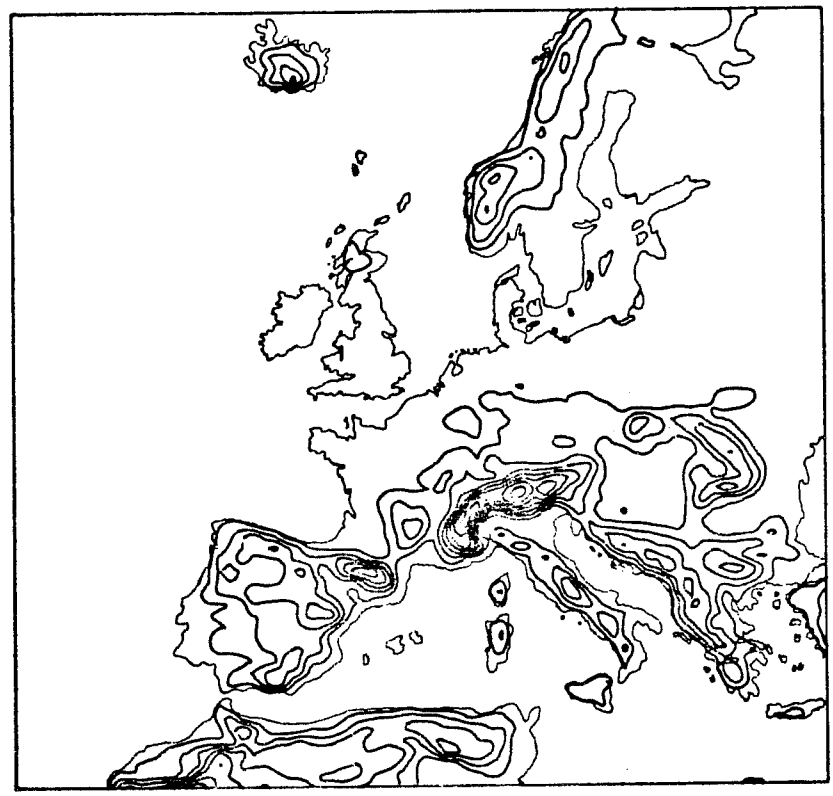

Fig.1 Orography of the Europa-Modell (contour interval 300 m).

The orography ϕ_s^{EM}, Figure 1, specially computed for this grid, is much steeper than the EC-orography; e.g. the maximum height difference between two neighbouring gridpoints is more than 1000 m in the EM-grid, but less than 500 m for the interpolated EC-orographies.

3. INTERPOLATION PROCEDURES

3.1 Interpolation of the mass field

The EC-mass field is defined by the surface geopotential ϕ_s^{EC}, the surface pressure p_s^{EC}, the temperature T^{EC}, and the relative humidity RH^{EC}. The transformation of the EC-mass field onto the EM-grid proceeds in four steps:

- Horizontal interpolation of ϕ_s^{EC}, p_s^{EC}, T^{EC}, and RH^{EC} from the N48-grid to the EM-grid; T63-fields are interpolated spectrally to the N48-grid prior to the transformation. Horizontally interpolated EC-fields are denoted by "$\sim$".
- Preliminary adjustment of the surface pressure p_s^{EM} to the EM-orography ϕ_s^{EM} based on the hydrostatic equation; p_s^{EM} determines the position of the 15 σ-type EM-levels.
- Vertical interpolation of $\tilde{T}^{EC}$ and $\tilde{RH}^{EC}$ to the EM-levels; the boundary layer profiles are treated separately.
- Final adjustment of the surface pressure p_s^{EM} to the EM-orography. This corrective step is very important for the proper relation between orography and surface pressure in the EM-grid.

The horizontal and vertical interpolations make use of 1-dimensional cubic splines under tension (De Boor, 1978). For smooth curves ordinary and tension splines correspond, but near steep slopes ordinary splines tend to oscillate and overshoot. Tension splines suppress this tendency depending on the tension factor which may vary between zero (no suppression) and infinity (straight line between the knots). The tension factor used here was 5.5.

The horizontally interpolated surface pressure $\tilde{p}_s^{EC}$ has to be corrected hydrostatically for the height difference $\Delta\phi_s = \phi_s^{EM} - \tilde{\phi}_s^{EC}$ between the EM-orography ϕ_s^{EM} and the interpolated EC-orography $\tilde{\phi}_s^{EC}$. For the N48-gridpoint model $\Delta\phi_s/g$ (g: constant of gravity) falls between -600 m and 1000 m, but about 90% of the height differences are within $\pm$ 200 m.

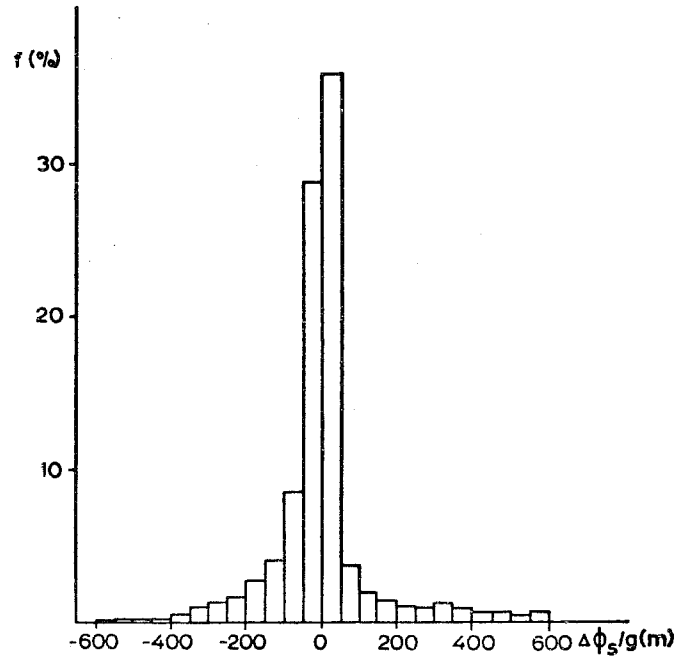

Fig.2a Histogram of the orography differences EM - EC (N48).

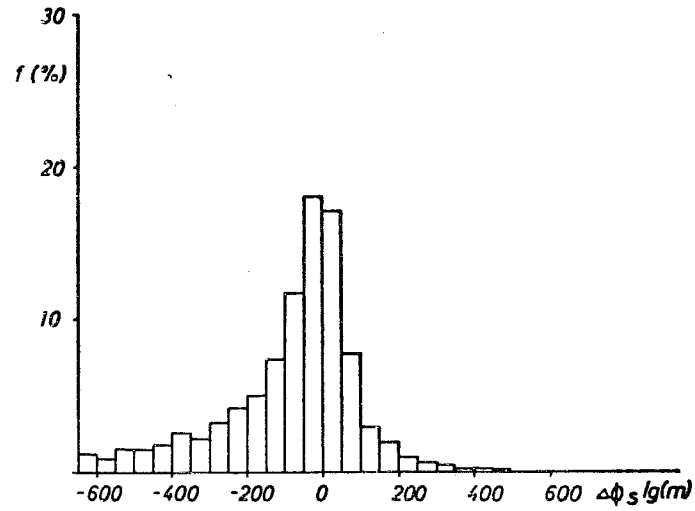

Fig.2b Histogram of the orography differences EM - EC (T63)

Figure 2a shows the histogram of the almost Gaussian distribution of the height differences between the EM-orography and the interpolated N48-orography.

The orography of the T63-model is of the envelope type, i.e. mean orography plus subgrid-scale variance. The height differences between the EM-orography and the interpolated T63-orography are greater, ranging from -1900 m to +800 m, and only 73 % fall between ± 200 m. The histogram, Figure 2b, is nega-

tively skew due to a mean difference value of approximately -120 m, whereas for the N48-orography the mean value is less than 0.2 m.

Computing the surface pressure p_s^{EM} at an EM-gridpoint is easy as long as the EM-orography is higher ($\Delta\phi_s > 0$) than the interpolated EC-orography. If the EM-orography is lower ($\Delta\phi_s < 0$), a profile of the virtual temperature has to be extrapolated. We use a linear regression for the virtual temperature T_v based on the lowest three (N48) or four (T63) EC-levels:

$$T_v = B \ln(p) + C \tag{1}$$

Inserting (1) into the hydrostatic equation (2)

$$d\phi = - R T_v d\ln(p) \tag{2}$$

yields an equation for p_s^{EM}:

$$p_s^{EM} = \exp\{[-C + \sqrt{C^2 + B(-2\Delta\phi_s/R + B(\ln(\tilde{p}_s^{EC}))^2 + 2C\ln(\tilde{p}_s^{EC}))}]/B\} \tag{3a}$$

and for B = 0 (isothermal atmosphere):

$$p_s^{EM} = \tilde{p}_s^{EC} \exp(-\Delta\phi_s/(R\,C)) \tag{3b}$$

where R is the gas constant.

The surface pressure p_s^{EM} based on Equation (3) is only preliminarily adjusted to the EM-orography and contains slight imbalances which we correct later. The errors stem mostly from the independent horizontal interpolation of the surface pressure p_s^{EC} and the surface geopotential ϕ_s^{EC}.

Using p_s^{EM} we perform the vertical interpolation of the temperature $\tilde{T}^{EC}$ and the relative humidity $\widetilde{RH}^{EC}$ to the EM-levels with tension splines. The computation tries to preserve the detailed boundary layer structure of the EC-data. We define the levels k = 13 to 15 (13 to 16 for T63-model) as "boundary layer" for the EC-analyses and k = 13 to 18 for the EM-model. When p_k^{EM} is greater than $\tilde{p}_s^{EC}$, the temperature and humidity profiles of the free EC-atmosphere are extrapolated linearly downwards to the top of the EM-boundary layer, where the EC-boundary

layer profiles are added. Figures 3a, b show the lower atmospheric temperature and humidity profiles for gridpoint (I = 58, J = 20) with a height difference $\Delta \phi_s/g$ = - 459 m.

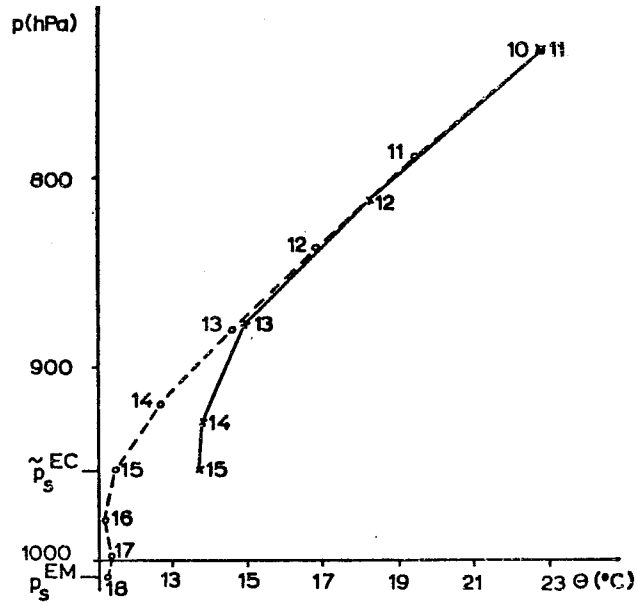

Fig.3a Profile of potential temperature at I = 58, J = 20, 12 UTC 1 March 1982.
x--x EC-data (horiz.interpolated), o--o EM-data.

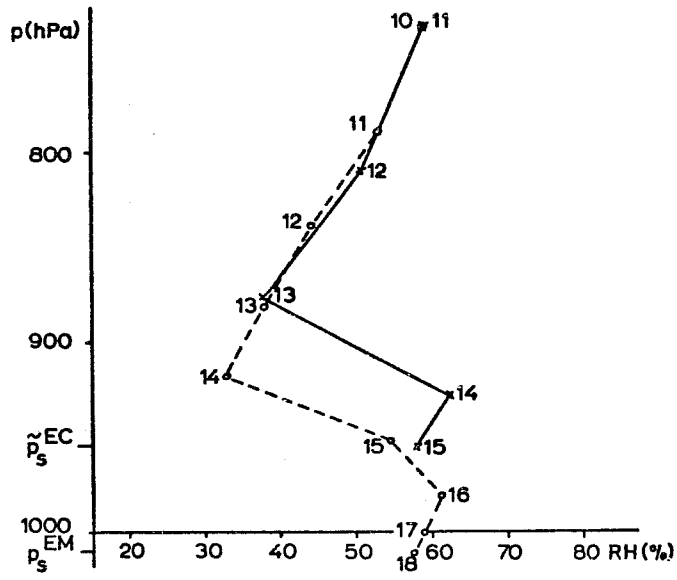

Fig.3b Same as Fig.3a, but for relative humidity.

If the EM-mountains are higher than the interpolated EC-mountains, the boundary layer structure is again transformed to correspond to the higher EM-surface. Figures 4a, b show the profiles of potential temperature and relative humidity for gridpoint (I = 52, J = 10) with a height difference $\Delta \phi_s/g$ = 432 m.

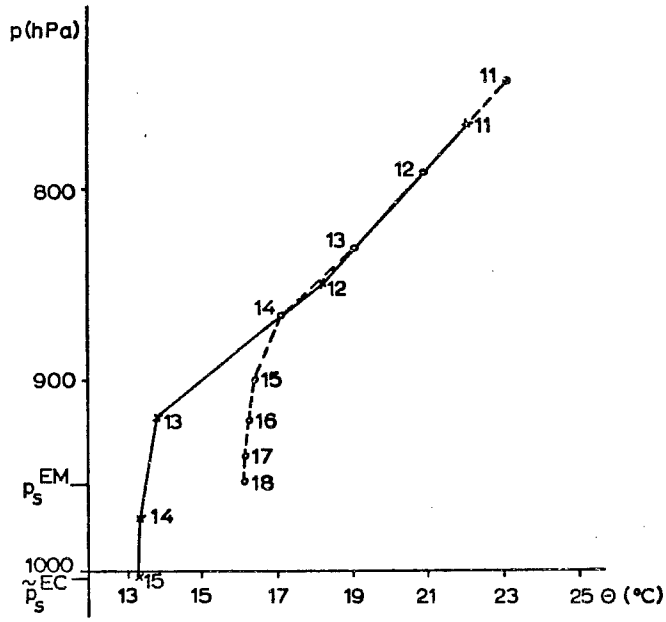

Fig.4a Same as Fig.3a, but at I = 52, J = 10.

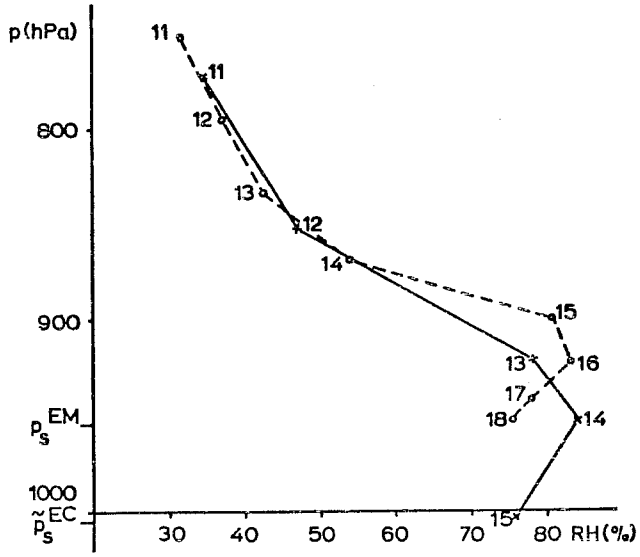

Fig.4b Same as Fig.4a, but for relative humidity.

To permit a consistent computation of the geopotential in the EM-grid, we correct the interpolated temperature profile above the boundary layer demanding that the layer-mean-temperature for fixed pressure intervals be the same for the EM- and the EC-stratification.

The final computation of the surface pressure p_s^{EM} corrects the above-mentioned slight errors. The correction is based on the following idea: We compute the geopotential ϕ^{EM}(600 hPa) of the 600 hPa-level, which is above the highest EM-mountains at all seasons. The same is done in the EC-grid using the original EC-surface pressure and virtual temperature. The geopotential ϕ^{EC}(600 hPa) is horizontally interpolated to the EM-grid. Since the geopotential ϕ^{EC}(600) is a smooth field compared with the rough surface pressure p_s^{EC}, the interpolation error is negligible. The difference $\Delta\phi(600) = \phi^{EM}(600) - \tilde{\phi}^{EC}(600)$ between the EM-geopotential and the horizontally interpolated EC-geopotential is attributed solely to errors in the preliminary computation of the surface pressure. The correction of p_s^{EM} necessary to minimize $\Delta\phi$(600) is quite small, normally less than 0.5 hPa, but may reach 2 hPa in the vicinity of steep slopes (e.g. the Alps). As a result, the changes in the height of the σ-type EM-levels are also small. We can thus neglect the slight variations in the interpolated temperature and relative humidity profiles. The final surface pressure p_s^{EM}, the interpolated temperature T^{EM}, and the relative humidity RH^{EM} represent a smooth transformation of the EC-mass field onto the EM-grid.

3.2 Interpolation of the wind field

The horizontal and vertical interpolation of the zonal and the meridional wind components, u^{EC} and v^{EC}, uses tension splines again. The wind profile is not extrapolated below the EC-orography, but the wind vector for EM-levels below the EC-surface is analyzed horizontally from surrounding gridpoints using a simple Cressman (1959) scheme.

The transformation to polar stereographic wind components u^{EM}, v^{EM} is as follows:

$$u^{EM} = \tilde{v}^{EC}\sin(\lambda_0 - \lambda) + \tilde{u}^{EC}\cos(\lambda_0 - \lambda),$$
$$v^{EM} = \tilde{v}^{EC}\cos(\lambda_0 - \lambda) - \tilde{u}^{EC}\sin(\lambda_0 - \lambda), \qquad (4)$$

with $\lambda_0 = 10^\circ$ E and longitude λ.

To adjust the wind field in the boundary layer (approximately the lowest five model layers) to the new surface parameters, e.g. the new roughness length, we use a method similar to the one proposed by Kurihara and Tuleya (1978). The solution of the stationary Ekman Equation (5) is considered to be the adjusted wind field.

$$f\,p^x(\mathbf{v} - \mathbf{v}_g)\,x\,\mathbb{K} + g\frac{\partial \pi}{\partial \sigma} = 0. \qquad (5a)$$

$$\pi = \begin{cases} g\rho^2/p^x K_M^v \dfrac{\partial \mathbf{v}}{\partial \sigma} & \text{Ekman layer} \\ -\rho_B C_M \mathbf{v}_P & \text{Prandtl layer,} \end{cases} \qquad (5b)$$

where $p^x = p_s^{EM} - p_T$ Surface pressure minus 250 hPa,
$\mathbf{v} = (u^{EM}, v^{EM})$ horizontal wind vector,
$\mathbf{v}_g$ geostrophic wind vector,
g constant of gravity,
π turbulent momentum fluxes,
K_M^v turbulent diffusion coefficient,
and C_M turbulent transfer coefficient.

The interpolated wind field in the boundary layer provides the initial guess for the iterative solution of Equation (5). The total mass field and the winds at the top of the boundary layer (level k = 13) remain constant. The turbulent fluxes are parameterized in the same way as in the EM-model (Müller, 1981).

Though the adjustment of the wind field works well for smaller mountains, it does not produce the proper flow around and across major mountain barriers as the Alps. The correct simulation of the dynamic effects of steep mountain chains fails because of the restriction on a fixed mass field. The final adjustment to the changed orographic forcing has to be accomplished during the first few hours of the forecast. During this time the model builds the stronger ridge upstream and the deeper trough downstream of the Alps, which are necessary for a correct dynamic

balance of the flow.

The interpolated wind in the free atmosphere and the adjusted boundary layer winds produce an unrealistically large initial pressure tendency $\frac{\partial p_s^{EM}}{\partial t}$ averaging 5 hPa/h and up to 60 hPa/h below the jet stream. A simple scaling of the tendency equation reveals the cause for the large tendency error. With a pressure tendency of 2 hPa/h the vertical mean divergence equals $6 \cdot 10^{-7} sec^{-1}$, but the divergence in a single layer may be up to $10^{-5} sec^{-1}$ or more. The vertical compensation of the divergence is very sensitive to small errors in the wind interpolation. To get a pressure tendency of 2 hPa/h, we have to interpolate the winds with an accuracy of approximately 0.05m/s which is impossible in situations with vastly different grids.

To remove the large external gravity wave which reflects the pressure tendency, we correct the divergent winds above the boundary layer requiring the corrected pressure tendency to equal the initial EC-tendency $\frac{\partial p_s^{EC}}{\partial t}$ interpolated on the EM-grid. This constraint yields an elliptic equation for the wind potential χ assuming a wind correction constant with height.

$$\left(\frac{\partial p_s^{EM}}{\partial t} - \frac{\partial \tilde{p}_s^{EC}}{\partial t}\right)/m^2 = \nabla^2 \chi \,(A(p_s^{EM} - p_T) + p_T) \; + A \nabla p_s^{EM} \cdot \nabla \chi$$

$$\text{with} \quad A = \sum_{k=1}^{18} w_k \, \Delta\sigma_k \qquad (6)$$

$$w_k = \begin{cases} 0 & k = 1,3 \\ 1 & k = 4,12 \\ 0 & k = 13,18 \end{cases} \qquad \text{weighting function}$$

where m is the map factor.

Equation (6) is solved with sequential overrelaxation under the assumption of a constant χ at the lateral boundaries of the domain. The absolute value of the wind correction $v_D = m \nabla \chi$ is usually less than 0.2 m/s, but may reach 2 m/s for a few points.

4. SELECTED RESULTS

4.1 Initial noise in the model

To demonstrate the impact of the normal mode initialization on the initial noise in the EM-model, we present some results of a forecast starting at 12 GMT on March 1, 1982. Initial and boundary values consist of interpolated EC-analyses, with updating of the boundary values every 6 hours and linear interpolation in time. The treatment of the lateral boundaries closely follows the method of Davies (1983) and Kallberg (1977); the boundary zone has a width of eight gridpoints. The steep Atlas mountain chain forms the southwestern boundary of the domain, with height differences of - 450 m up to 1000 m (N48) and - 1000 m up to 600 m (T63) between the EM- and the interpolated EC-orographies, although LAM-modellers normally avoid placing a boundary in an area with a vastly different orography (Miyakoda and Rosati, 1977).

The area-averaged absolute value of the surface pressure tendency is a sensitive measure of the activity of gravity waves in a model. Figure 5a shows the pressure tendency during the first

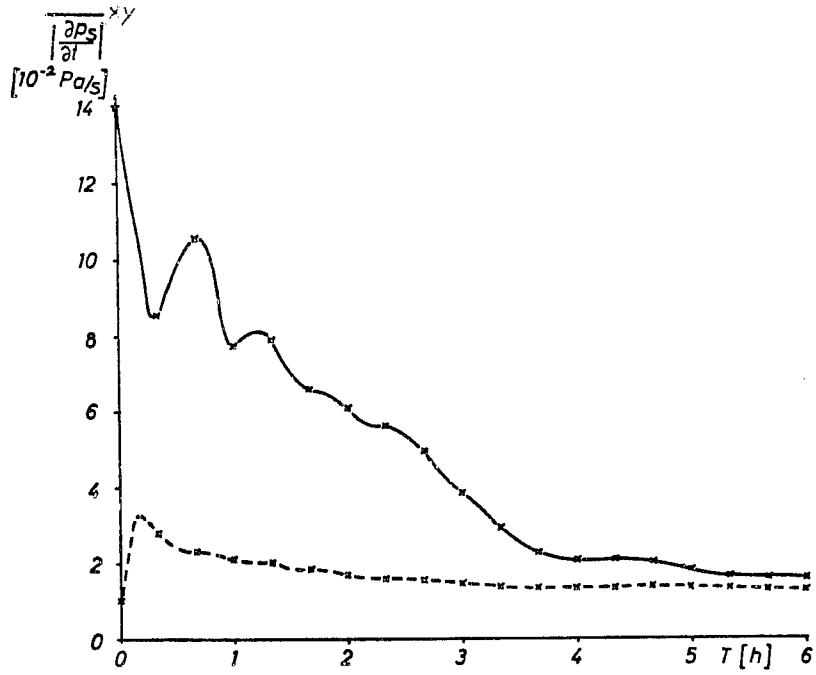

Fig.5a Area-averaged surface pressure tendency without (—) and with (--) normal mode initialization.

six hours of the forecast. The continuous line results from the uninitialized global EC-analysis, the dashed line corresponds to the initialized EC-analysis. The uninitialized analysis produces a strong shock to the EM-model with a high level of gravity wave activity. The interpolation of the initialized analysis preserves the balanced state to a high degree, though there is an initial increase in the noise level. But the gravity waves possess only small amplitudes and high frequencies, as demonstrated in Figure 5b, which shows the pressure tendency when the Edelmann (1978) averaging scheme is applied. The prognostic variables, surface pressure, wind, enthalpy, and mixing ratio for water vapour and cloud water, are averaged over a period of N timesteps ΔT (N = 24, ΔT = 75 sec). The model is restarted at timestep N/2 using the averaged variables as initial values. Obviously the very short averaging period of 24 timesteps (0.5 hour) is sufficient to remove most of the high frequency noise generated by the interpolation of the initialized EC-analysis. However, the averaging period is much to short to dampen efficiently the noise in the uninitialized case because the period of the gravity oscillations is longer than 0.5 hours.

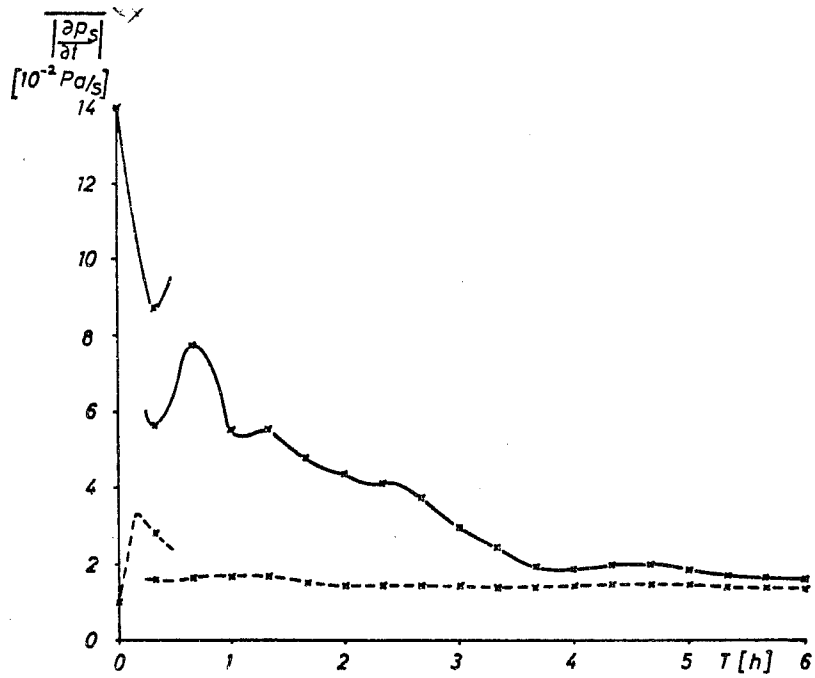

Fig.5b Same as Fig.5a, but including Edelmann's averaging scheme.

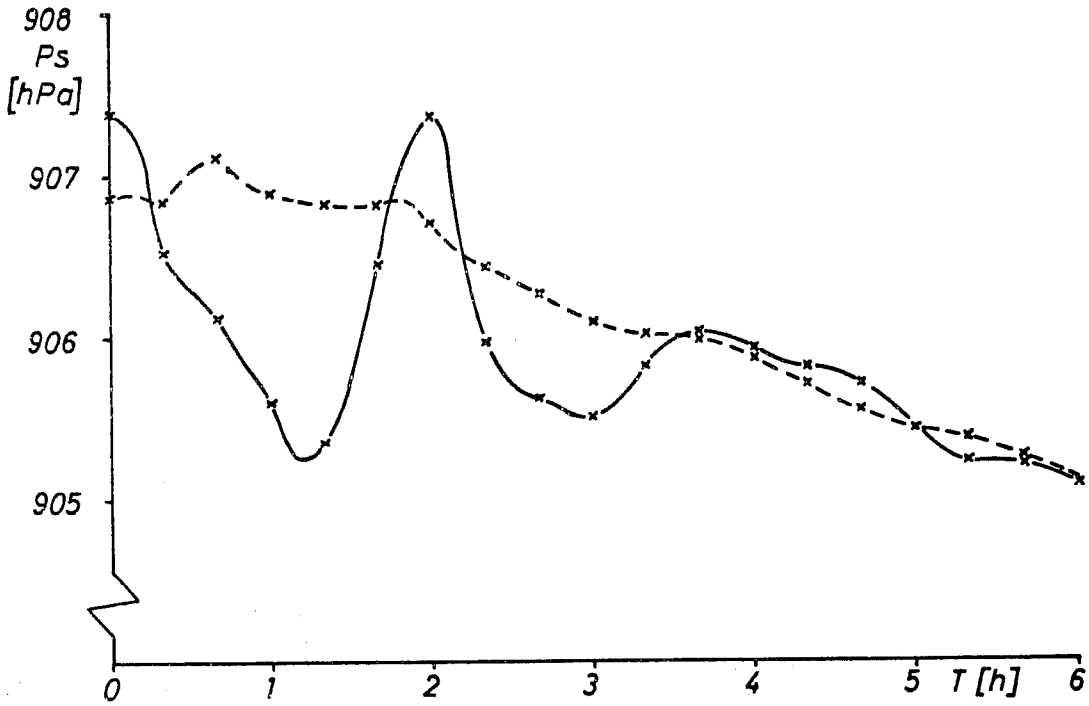

Fig.6 Surface pressure at I = 45, J = 25 (Zürich) without (—) and with (--) normal mode initialization.

Figure 6 shows the time-trace of the surface pressure for grid-point (I = 45, J = 25) near Zürich (Alps). The uninitialized forecast (solid line) is contaminated by oscillations which have an amplitude of 1 hPa and a period of 2 hours, and die away with time. After three to four hours most of the initial

gravity waves have left the forecast domain and the curve approaches the smooth graph of the initialized forecast. Thus the velocity of the gravity waves is about 200 to 300 m/s. If the boundary treatment inhibits the gravity waves leaving the domain, the noise level remains high.

4.2 Spin-up time of vertical velocity and precipitation

Comparing the area-averaged vertical velocities for three forecasts starting 12 hours apart on March 1, 1982, 12 GMT, on March 2, 1982, 00 GMT, and on March 2, 1982, 12 GMT, the spin-up time of the LAM's circulation can be measured. Figure 7 shows the vertical velocity for three levels, at the top of the boundary layer (k = 13), at 660 hPa (k = 9), and near the jet level (k = 4).

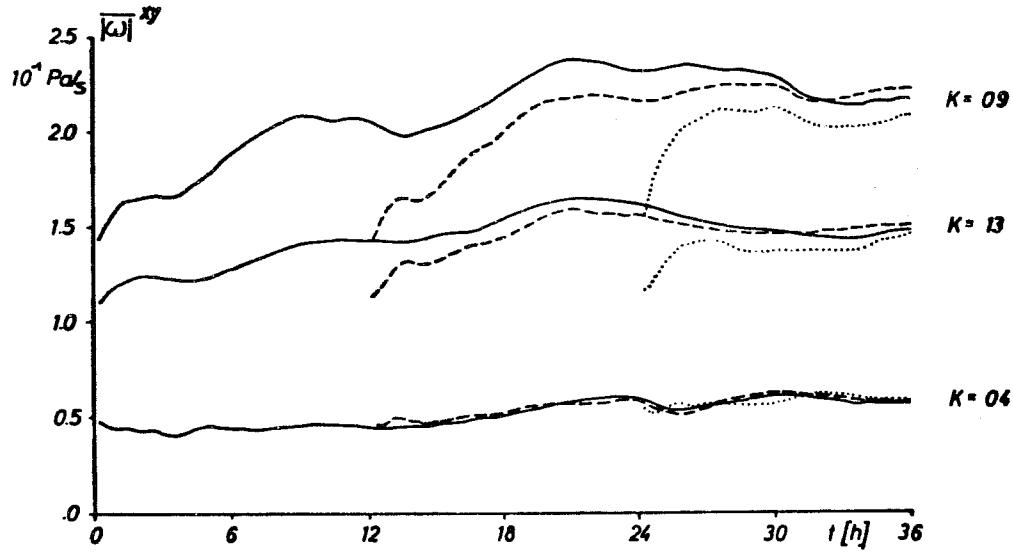

Fig.7 Adaption of vertical velocity at levels k = 4, 9 and 13. Forecasts starting at 12 UTC 1 March 1982 (—), 00 UTC 2 March (--), and 12 UTC 2 March (...).

Because of the normal mode initialization the vertical velocity has reasonable initial values and needs only between two and three hours to reach equilibrium values consistent with the LAM's forcing. The precipitation rate, Figure 8, needs a similar adjustment time.

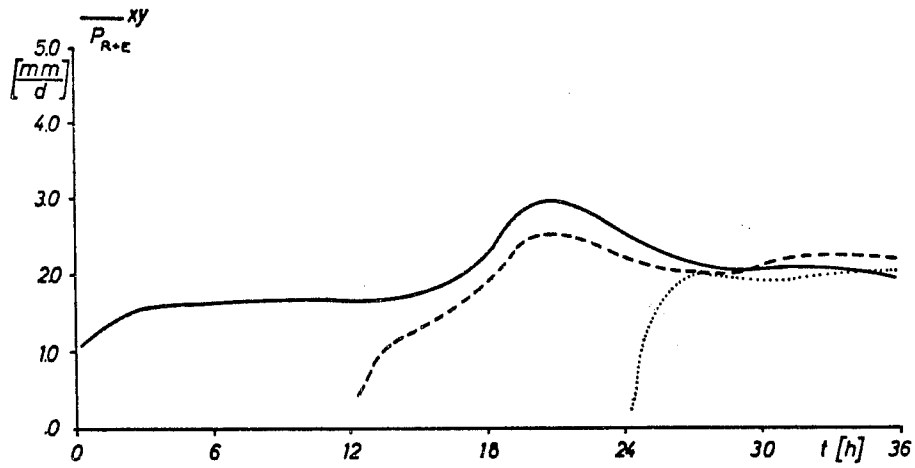

Fig.8 Same as Fig.7, but for precipitation.

4.3 Spectral decomposition of the difference fields EM-EC

In the course of the forecast the EM-model generates meso-scale structures with shorter wavelength than the EC-model data. To gain insight into this process we made a spectral analysis of the difference fields between an EM-forecast and the corresponding EC-forecast. The EC-forecast on model levels was kindly provided by the ECMWF. Because the interpolated EC-forecast data were used as boundary values for the EM-forecast in this case study, the difference fields vanished at the boundaries due to the boundary treatment. The (EM - EC)-flow is thus representable in terms of pure sine functions. The squared amplitude of each Fourier component is a measure of the energy of that wave. For the EM-domain of 73 x 69 gridpoints there are 71 x 67 spectral coefficients for each field and level. In order to distinguish between synoptic and sub-synoptic flow pattern we divide the spectral space into two parts. One (LS) represents the large-scale differences with a wavelength greater than 600 km, the smallest features, the EC-model can resolve. The other (MS) is the meso-scale difference with a length scale in one (or both) directions of less than 600 km. The square root of the sums of the squared Fourier coefficients in the LS- and MS-part of the spectral space are shown in Figure 9a,b,c,d, and e for a 48 hour-forecast starting on March 1, 1982, 12 GMT. The time-traces of the summed meso-scale amplitudes (MS) for

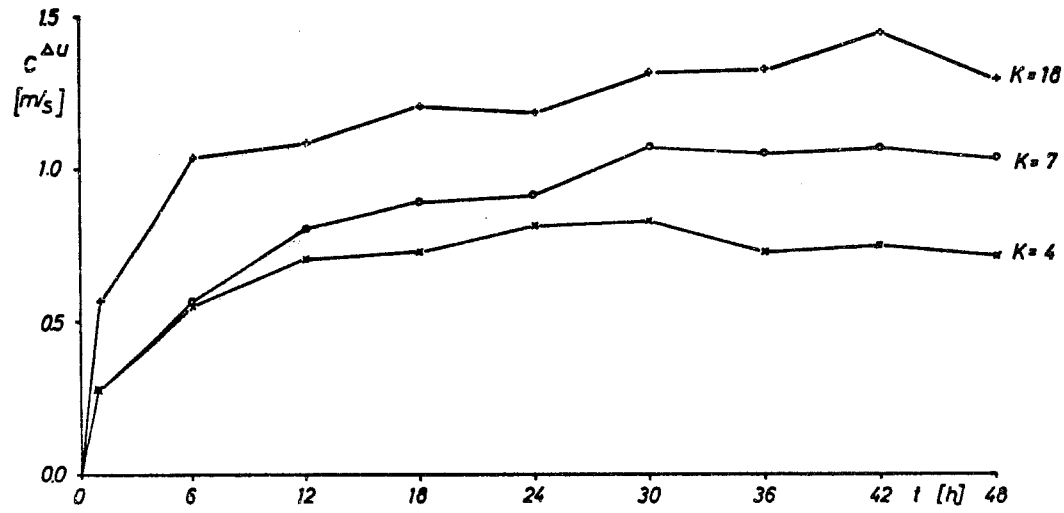

Fig.9a Meso-scale part of the difference field (EM - EC) for the zonal wind at levels k = 4, 7 and 18.

the zonal wind u, Figure 9a, at the levels k = 4 (290 hPa), k = 7 (500 hPa), and k = 18 (about 30 m above the ground level) prove that the MS-part of the flow is strongly forced by the ground and to a lesser extent by scale interaction. The magnitude of the difference (EM - EC) is inversely proportional to the height of the layer. The model needs between 6 and 18 hours to reach quasi-equilibrium values for the MS-part of the flow. The rather long adjustment time is partly caused by the lack of a diurnal cycle in the EC-model at that time.

Figures 9b,c,d, and e compare the MS- and LS-part of the difference fields at level k = 13 (about 850 hPa) for the zonal wind u, the enthalpy h, the water vapor mixing ratio q_{DW}, and the surface pressure p_s. While for u, h, and q_{DW}, MS and LS have the same magnitude, the LS-part of the surface pressure dominates the MS-part. The observed drift of the LS-differences reflects either a better simulation of the large-scale flow due to resolved meso-scale circulations which were parameterized in the EC-model, or the well-known problem LAMs have in simulating properly the mass flow through the open boundaries. We have to study more cases to solve this problem finally.

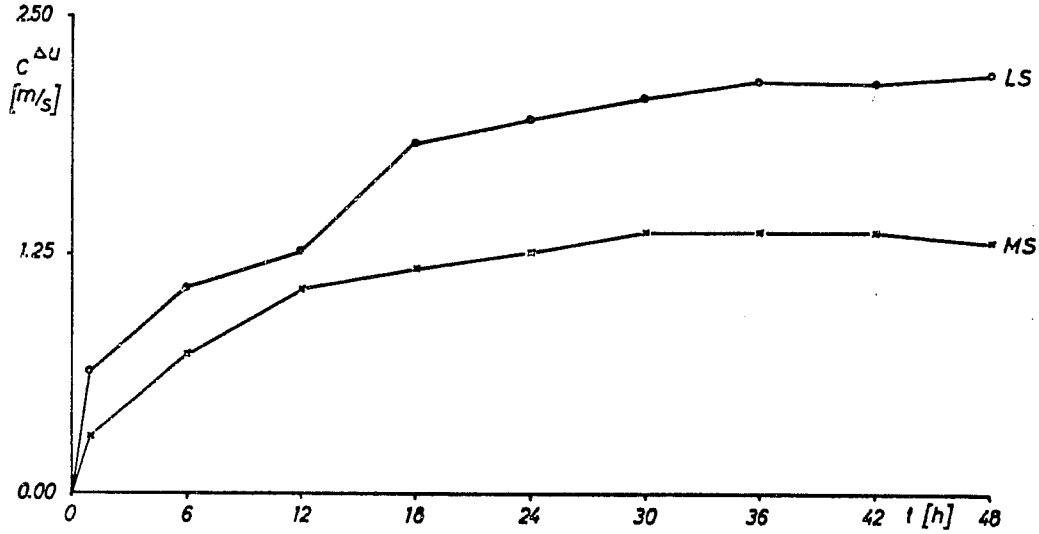

Fig.9b Meso-scale (MS) and large-scale (LS) part of the difference field (EM - EC) for the zonal wind at level k = 13.

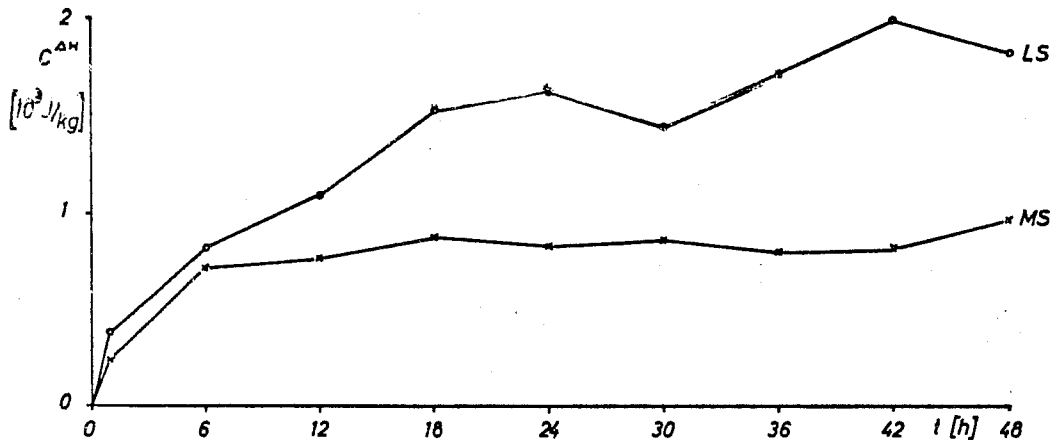

Fig.9c Same as Fig.9b, but for enthalpy.

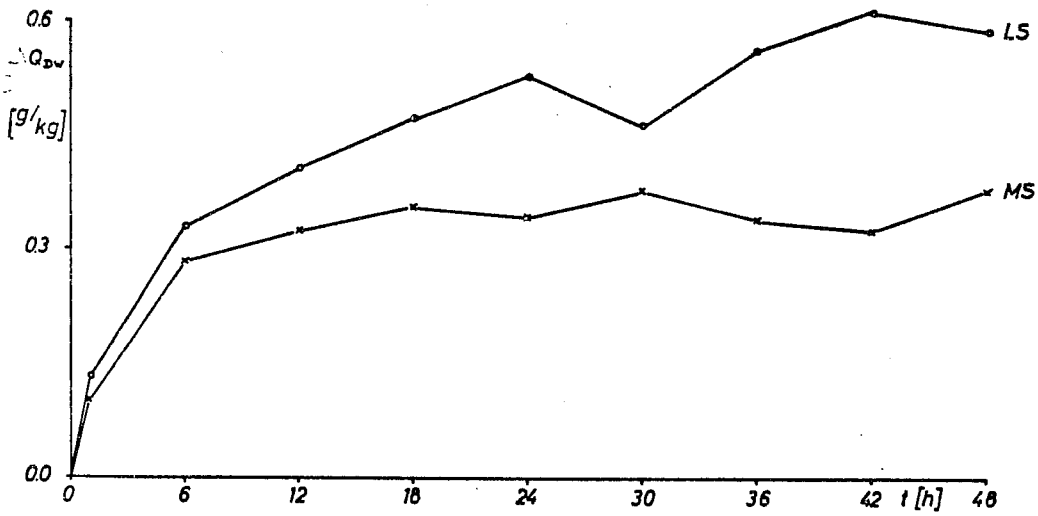

Fig.9d Same as Fig.9b, but for mixing ratio.

Fig.9e Same as Fig.9b, but for surface pressure.

Because of the long time (6 to 18 hours) needed for the full development of the MS flow from LS initial conditions, a careful initialization of the meso-scale circulation systems is urgent. The high resolution analysis should preserve as much as possible the meso-scale structures generated by the model.

4.4 Spin-up time of topographically induced circulations

On March 2, 1982 a strong northerly flow hit the Alps behind a southeastward moving coldfront. Strong mountain waves were observed in the lee of the Alps over the Po valley. An EM-forecast was initialized on March 2, 1982, 12 GMT and cross-sections from Stuttgart (Germany) to Tunis (North Africa) were made after 1 hour, 3 hours and 5 hours forecast time, Figures 10b, c and d. Figure 10a shows the smooth initial relative humidity (interpolated EC-analysis), which is not yet adapted to the steeper EM-Alps. Only one hour later, Figure 10b, the EM-model generated the cloud system typical of "Föhn" situations like this. North of the Alps a massive cloud shield developed due to the forced lifting on the windward side of the Alps and a strong downdraft in the lee created a dry zone over the Po valley. The islands in the Mediterranean have a similar influence on a smaller scale. After 3 hours, Figure 10c, the adaption process reaches a quasi-equilibrium.

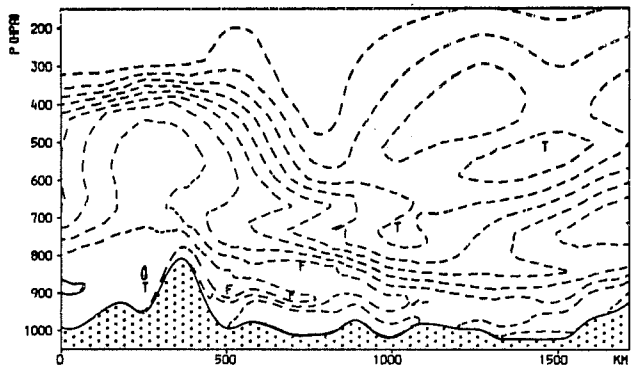

Fig.10a EC-analysis (interpolated onto EM-grid) of relative humidity (contour interval 10%) 12 UTC 2 March 1982.

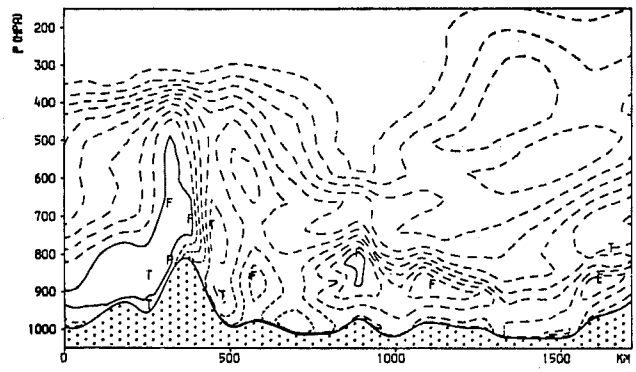

Fig.10b EM-forecast of relative humidity (contour interval 10%) 12 UTC 2 March 1982 + 1 hour.

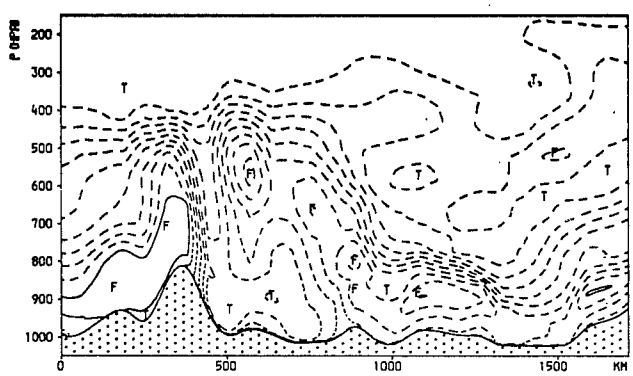

Fig.10c Same as Fig.10b, but + 3 hours.

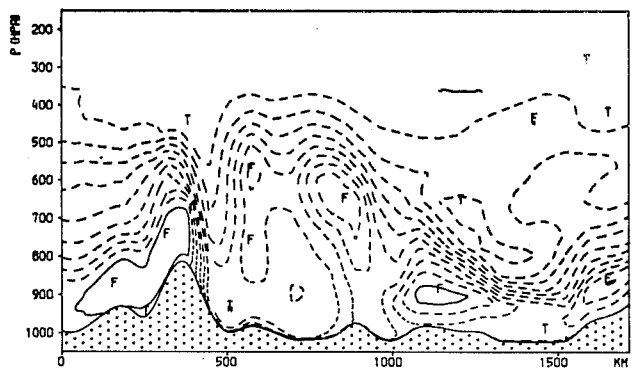

Fig.10d Same as Fig.10b, but + 5 hours.

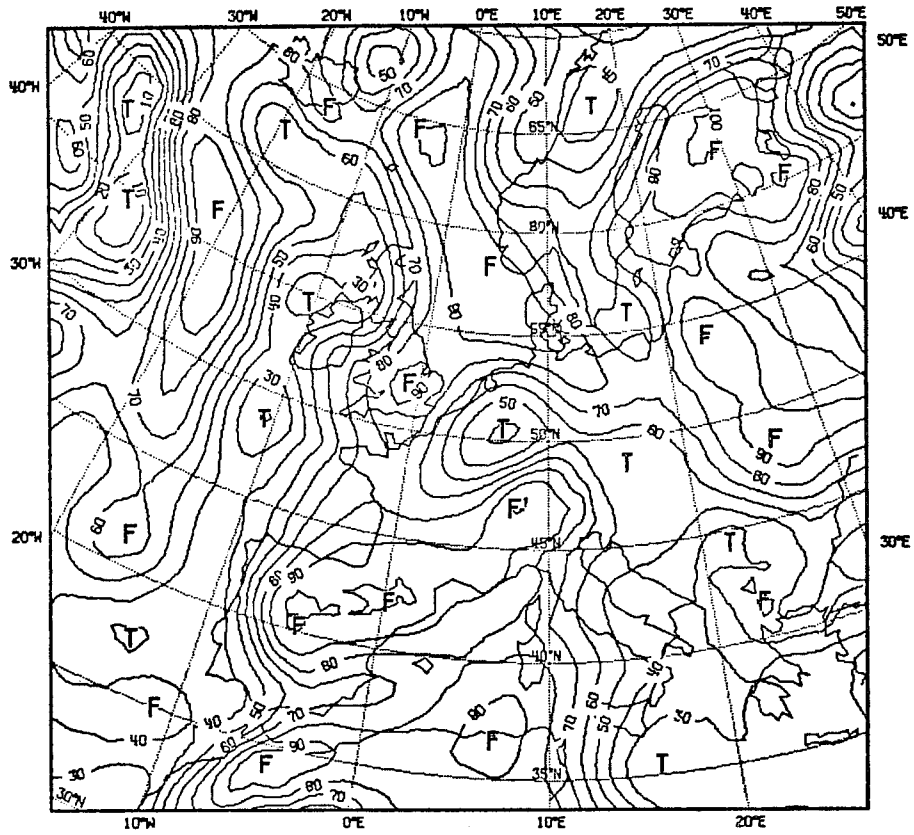

Fig.11a EC-analysis of relative humidty at 700 hPa, 00 UTC 29 September 1984.

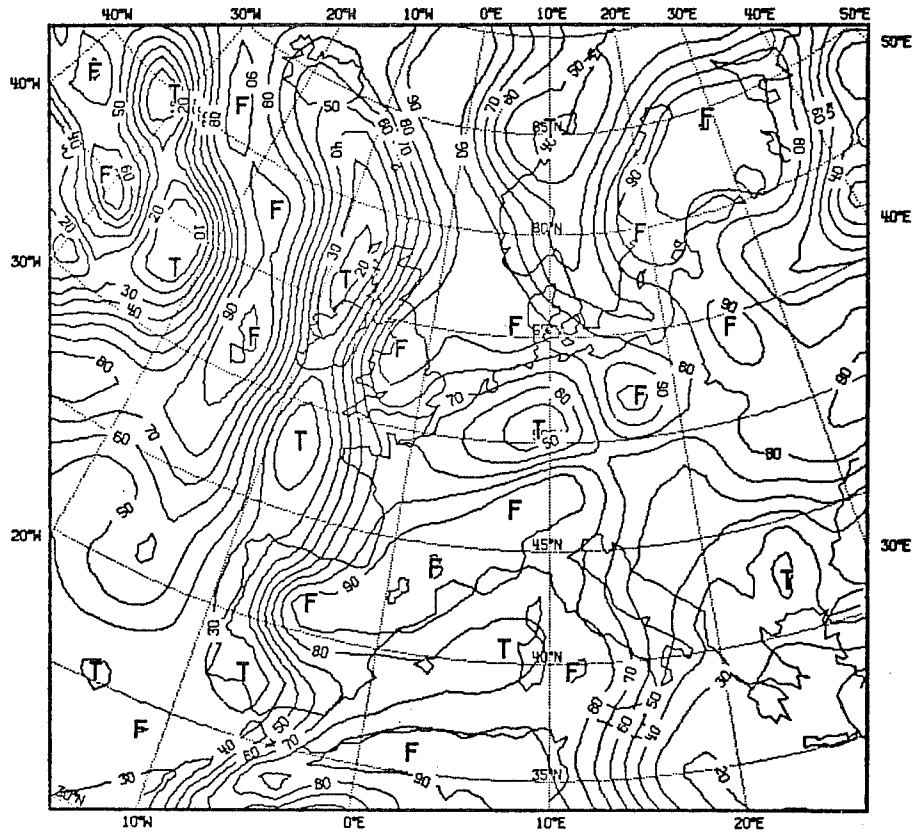

Fig.11b Same as Fig.11a, but for 06 UTC 29 September 1984.

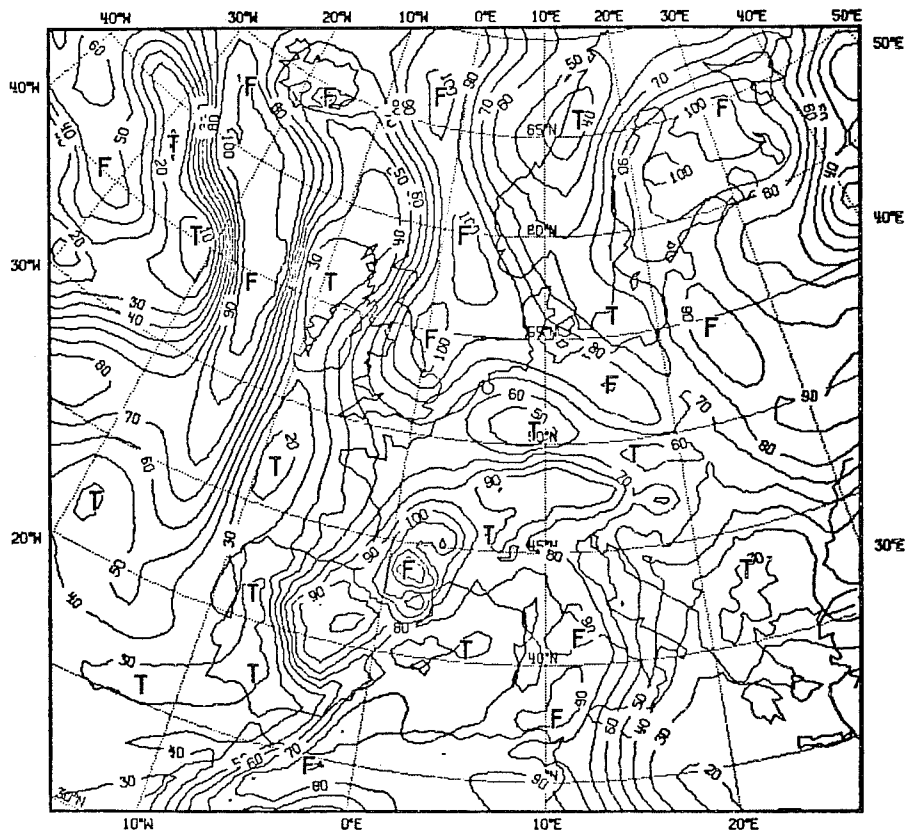

Fig.11c EM-forecast (+ 6 hours) of relative humidity at 700 hPa, valid 06 UTC 29 September 1984.

Comparing the 3-hour-flow with the situation after 5 hours (Figure 10d), we notice only slight changes in the humidity distribution.

4.5 Increase of gradients by scale interaction

The high resolution of the EM-model allows a better representation of frontal gradients in the flow. On September 29, 1984, 00 GMT a coldfront is slowly moving eastward over the North Sea and France accompanied by waves over East England and the Gulf of Lions. The initial relative humidity at 700 hPa is shown in Figure 11a. The two waves lead to humidity values greater than 90 % over Middle England, the North Sea and southern France.

Six hours later, at 06 UTC, Figure 11b, the situation remains almost unchanged in the analysis. The EM-model, starting at 00 GMT, computes for 06 UTC the humidity distribution in Figure 11c. The waves are clearly discernable in humidity values well above 100 % and the humidity gradient across the front is much better resolved. The frontal system west of Ireland has sharper boundaries too. Obviously, a 6-hour EM-forecast suffices to develop quite realistic cross-frontal gradients in spite of rather smooth initial fields.

5. Concluding remarks

Interpolated initialized large-scale analyses provide a limited area meso-scale model with initial and boundary values. The proposed interpolation techniques preserve the balanced state of the initialized large-scale data rather well. The model generates meso-scale flow systems in the course of the forecast resulting from lower boundary forcing and scale interaction. Depending on the type of the meso-scale structure the adjustment time is between 3 and 18 hours, but after 6 to 12 hours the EM-forecast contains much more detail than the corresponding large-scale analysis.

The design of a high resolution analysis scheme should take these results into account. Balanced initial values are desirable for very short range forecasts (less than 6 hours) and update intervals of 3 hours in 4-dimensional data assimilation. The best balance of the large-scale flow is achieved by global normal mode initialization. Thus a high resolution analysis should be able to transform the balanced flow smoothly from the large-scale to the meso-scale grid. If the first guess of the high resolution analysis consisted at least partly of the corresponding large-scale analysis, this constraint could be satisfied. On the other hand, we should try to analyze as many meso-scale flow patterns as possible because of the rather long spin-up times of up to 18 hours. Since some of the meso-scale features created in the model will most certainly not be observable by routine measurements (e.g. mountain waves, boundary layer flow), the analysis should try to preserve this information. It is therefore tempting to propose the use of a suitable linear combination of interpolated large-scale analysis and a short range (6 to 12 hours) meso-scale forecast as first guess for the high resolution analysis.

References

Atkinson, B.W., 1981: Meso-scale atmospheric circulations. Academic Press, London, New York, 495pp.

Bengtsson, L., 1984: Medium-range forecasting at ECMWF; a review and comments on recent progress. Long and medium range weather forecasting. Ed. D.M. Burridge and E. Kallèn, Springer-Verlag, 274pp.

De Boor, C., 1978: A practical guide to splines. Springer-Verlag, New York, 392pp.

Cressman, G.P., 1959: An operational objective analysis system. Mon.Wea.Rev., 87, 367-381.

Davies, H.C., 1983: Limitations of some common lateral boundary schemes used in regional NWP models. Mon.Wea.Rev., 111, 1002-1012.

Dell'Osso, L., 1983: High resolution experiments with the ECMWF model: A case study. ECMWF Technical Report No. 37, 53pp.

Edelmann, W., 1978: Die Vorhersagemodelle des DWD. Fortbildungsvorträge zur numerischen Wettervorhersage, 58pp.

Hoke, J., N.A. Phillips and J.G. Sela, 1983: Normal mode initialization of the nested grid model of the National Meteorological Center. Sixth Conference on Numerical Weather Prediction, 152-158; AMS.

Lorenc, A., 1981: Design of ECMWF analysis scheme. Seminar 1980, Data Assimilation Methods, ECMWF, Reading, U.K., 83-106.

Kallberg, P., 1977: Test of a lateral boundary relaxation scheme in a barotropic model. ECMWF Interal Report.

Kurihara, Y. and R.E. Tuleya, 1978: A scheme for dynamic initialization of the boundary layer in a primitive equation model. Mon.Wea.Rev., 106, 113-123.

Miyakoda, K. and A. Rosati, 1977: One-way nested grid models: The interface condition and the numerical accuracy. Mon.Wea. Rev., 105, 1092-1107.

Müller, E., 1981: Turbulent flux parameterization in a regional-scale model. ECMWF Workshop on planetary boundary layer parameterization, 193-220.